Evaluation of Some Designed Halogenated Variants of Gentisyl Alcohol: Molecular Docking, DFT, Druglikeness, and ADMET Studies for Assessing Biological Properties

**Basanta Singha, Partha Pratim Gogoi , Penlisola Longkumer, Nichan Boruah and Upasana Bora Sinha***

Department of Chemistry, Nagaland University, Lumami-798627, Nagaland, **INDIA**
Email: upasanabsinha@gmail.com

_____

ABSTRACT

Antimicrobial resistance (AMR) poses a significant threat, complicating infection treatment and increasing the risks of severe illness. Concurrently, inflammation, prevalent in health issues like cardiovascular diseases, cancer, and diabetes, necessitates more effective therapeutic strategies. This dual challenge of AMR (Anti-microbial resistance) and inflammation underscores the critical need for novel and effective therapeutic. Incorporating halogen atom can profoundly alter a molecule's properties and may influence its bioactivity, metabolism, and pharmacokinetic profile. This study thus aims to design variants of gentisyl alcohol by incorporating bromine, fluorine, chlorine, and iodine atoms, evaluating their potential as antibacterial, anti-tubercular, antiviral, anti-parasitic, and anti-inflammatory agents via computational means. Employing molecular docking and Density Functional Theory (DFT), we assessed binding affinity, reactivity, and stability, alongside drug-likeness, pharmacokinetics, and toxicity. Compounds 7F, 4F, 7Br, 1F, and 7I exhibited superior and highest docking scores compared to gentisyl alcohol and native ligands against the target of interest with respect to PDB ID 7DQL, 3O4M, 4YRE, 7NNY, and 7OFS. Similarly DFT analysis revealed lower HOMO-LUMO energy gaps, suggesting enhanced and better stability and reactivity. These compounds met druglikeness criteria, demonstrated favorable ADME/T properties, and exhibited no signs of toxicity, indicating promise for drug development. Their high gastrointestinal absorption, moderate skin permeability, and absence of P-glycoprotein substrate activity further support their potential as lead compounds. In conclusion, compounds 7F, 4F, 7Br, 1F, and 7I shows potential in possessing broad-spectrum bioactivity and thus warrants further exploration and optimization for therapeutic applications.

Graphical Abstract:
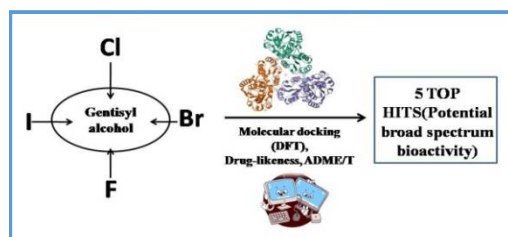
Gentisyl Alcohol: Halogenated Variant's Molecular Docking,
DFT, Druglikeness, and ADMET Assessment

_____

_____

INTRODUCTION

According to the World Health Organization (WHO) infectious diseases stemming from bacteria, viruses, and parasites constitute a significant cause of human mortality, contributing to approximately 25% of all disease-related deaths [1]. The pace of antibiotic development has notably fallen behind the rapid emergence of bacterial drug resistance. Concurrently, since the onset of the 21st century, the world has witnessed the emergence of novel viral infections such as H1N1 influenza, Ebola, Zika poliomyelitis, and COVID-19, leading to numerous Public Health Emergencies of International Concern [2]. Antimicrobial resistance (AMR) arises when bacteria, viruses, fungi and parasites undergo evolutionary changes over time, rendering the unresponsive to antibiotics. This phenomenon complicates the treatment of illnesses heightening the risk of disease transmission, severe illness, and mortality. AMR typically develops through natural genetic mutations driven by natural selection. The emergence of drug resistance renders antibiotics and other antimicrobial medications ineffective, making infections increasingly challenging or even impossible to treat [3]. Undoubtedly, chronic inflammatory diseases stand out as the leading cause of global mortality presently, accounting for over 50% of all fatalities. These diseases are characterized by inflammation and include conditions such as ischemic heart disease, stroke, cancer, diabetes millitus, chronic kidney disease, non-alcoholic fatty liver disease (NAFLD), as well as autoimmune and neurodegenerative disorders [4, 5]. from this standpoint, it's evident that there's a pressing demand for the exploration and creation of new antibiotics, alongside the advancement of innovative antimicrobial and anti-inflammatory agents. the average cost of developing an effective drug ranges from $900 million to $ 2 billion, factoring in numbers failures. Only one in 10,000 compounds make it to market, and of those just one in three recoups its development costs. This highlights the significant risk inherent in drug development [6]. Amid challenges, modern drug discovery utilizes innovative techniques like computer-aided drug design (CADD), including *in sillico* method, bioinformatics, cheminformatics, and quantum calculations. Advancements in computational techniques and hardware have enabled leading pharmaceutical companies and research groups to expedite the drug discovery process [7].
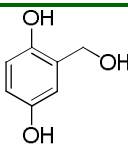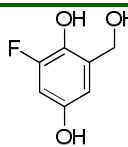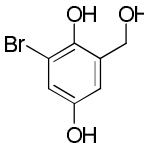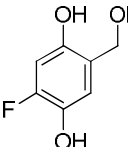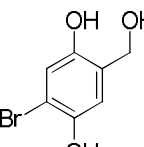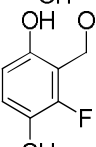
CADD methodologies are increasingly vital in drug discovery, offering cost-effective identification of promising drug candidates. These computational methods reduce reliance on animal models, aid rational design of safe drugs, and support drug repositioning. They provide crucial assistance to medicinal chemists and pharmacologists [8]. Halogen bonding is pivotal in drug discovery and design, with extensive applicability. Halogens like fluorine, chlorine, bromine, and iodine (represented as X) are essential ligand substituents in pharmacology. They are prevalent in approximately half of all molecules screened through high-throughput methods and are found in about 40% of drugs either on the market or in clinical trials. Furthermore, around a quarter of medicinal chemistry literature and patents involve adding halogen atoms in later synthesis stages [9-12]. The intentional utilization of halogen bonding as a potent tool, akin to hydrogen bondin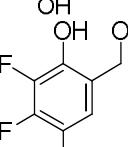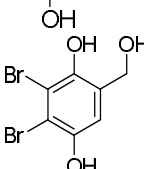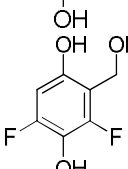g, holds promise for enhancing binding affinity and influencing binding selectivity. The rational design of potent inhibitors against therapeutic targets *via* halogen bonding remains an intriguing field, set to be further explored through a combination of experimental techniques and theoretical calculations in the future [13]. Machine Learning emerges as a valuable asset in this domain, offering diverse tools and techniques that significantly enhance the discovery process and decision-making capabilities. This is particularly beneficial for well-defined questions with ample high-quality data available [14]. Thus, this study focuses on designing derivatives of gentisyl alcohol [15] by strategically incorporating bromine, fluorine, chlorine, and iodine atoms. The objective is to evaluate their potential as antibacterial, anti-tubercular, antiviral, anti-parasitic, and anti-inflammatory agents. Computer-aided *in silico* techniques, such as molecular docking study, were employed to assess their binding affinity against the respective targeted diseases using a docking approach called redocking, involving the native and co-crystallized ligands. Subsequently, compounds with the highest docking scores against
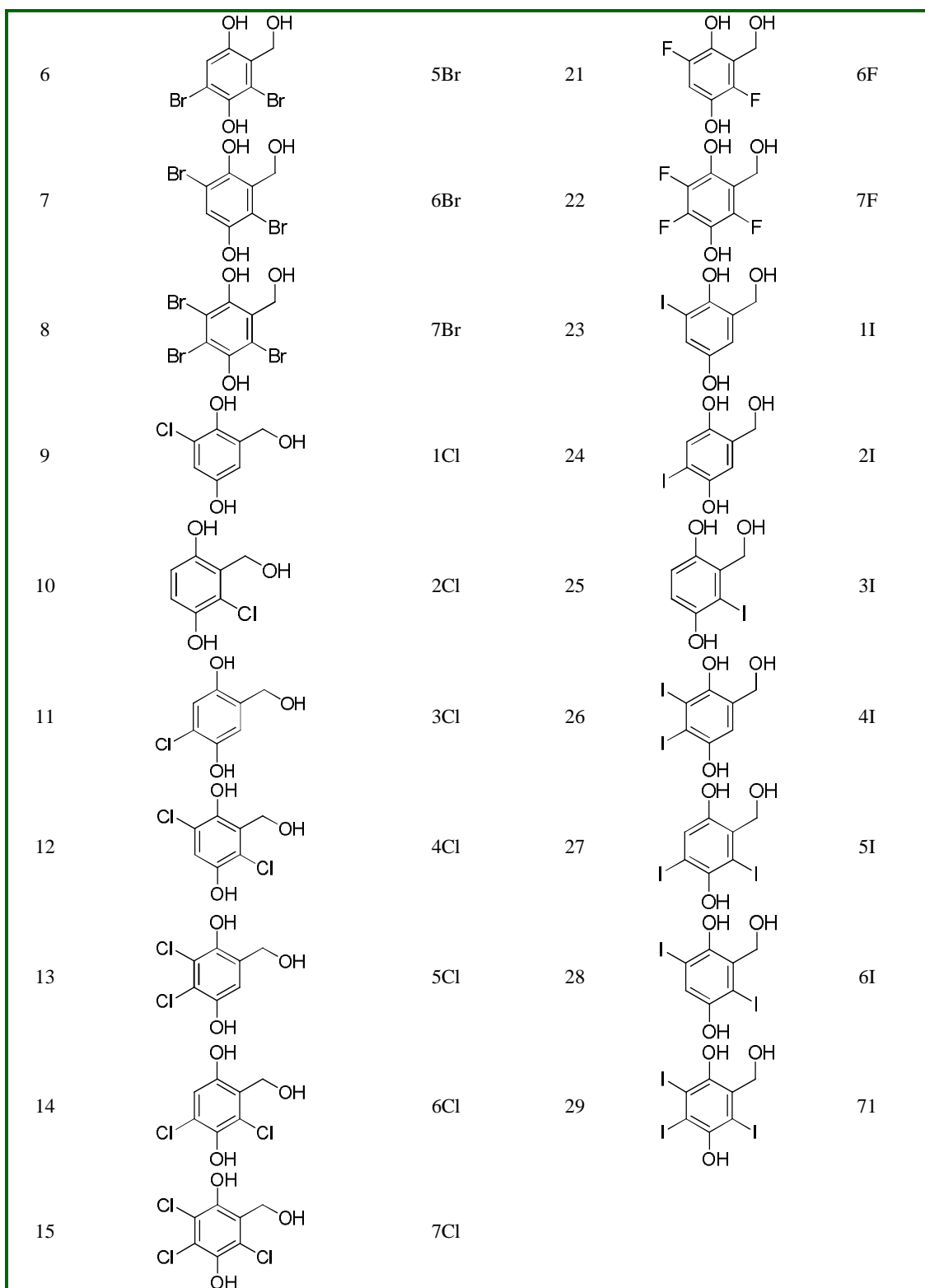
the respective targets undergo Density Functional Theory (DFT) study to evaluate their reactivity and stability. Furthermore, drug-likeness, pharmacokinetics, and toxicity screening are conducted to determine whether they possess drug-like and pharmacological characteristics and assess their potential as lead therapeutics.

MATERIALS AND METHODS

Compounds in focus: The compounds investigated, as shown below in table 1, were designed from gentisyl alcohol, strategically incorporating bromine (Br), chlorine (Cl), and fluorine (F) substitutions at the unoccupied ortho and meta positions of the parent compound. This substitution strategy presents a versatile approach for modulating the chemical properties and reactivity of the resulting compounds, thereby broadening their potential applications across diverse scientific domains such as pharmaceutical research, materials science, and organic synthesis [16]. With the exception of compound codes 1Br, 3Br, 1Cl, 2Cl, 3Cl, 2F, 1F, and the parent gentisyl alcohol, which are documented in ChemSpider (http://www.chemspider.com) and PubChem (https://pubchem.ncbi. nlm.nih.gov) databases, the remaining compounds, were designed via halogen substitution. The set of compounds or ligands shown in table 2 are the co-crystallized ligands present on PDB IDs. Using the native-co-crystallized ligand as a reference for comparing docking affinity against new ligands is crucial in computational docking studies for various reasons. Firstly, it serves as a validation tool for the docking methodology by assessing the accuracy in reproducing binding modes and affinities. Secondly, it aids in evaluating the binding site's suitability for different ligands, indicating its adaptability and consistency. Thirdly, it helps in identifying ligand similarities, facilitating ligand optimization and SAR studies. Additionally, it allows for the benchmarking of predicted affinities and provides context to the results obtained for new ligands, thereby enhancing the reliability and interpretability of computational simulations for rational drug design and lead optimization [17].

Table 1. List of compounds understudy and their compound code

S. No	Compounds	Compound Code	Sl. No	Compounds	Compound Code
1		Gentisyl alcohol	16		1F
2		1Br	17		2F
3		2Br	18		3F
4		3Br	19		4F
5		4Br	20		5F

6		5Br	21		6F
7		6Br	22		7F
8		7Br	23		1I
9		1Cl	24		2I
10		2Cl	25		3I
11		3Cl	26		4I
12		4Cl	27		5I
13		5Cl	28		6I
14		6Cl	29		7I
15		7Cl			
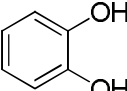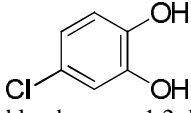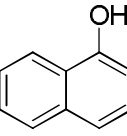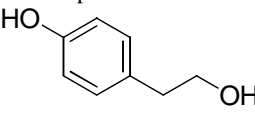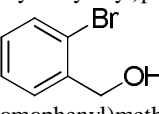
Molecular docking

Selection of targets: The crystal structures of all the targets were obtained from the Research Collaboratory for Structural Bioinformatics (RCSB) Protein Data Bank (PDB) (http://www.rcsb.org/). Targets of interest with respect to bacterial, inflammation, parasitic, tubercular, and viral consist of PDB ID 7DQL (E. coli GyrBATPase domain in complex with 4-chlorobenzene-1,2-diol) [18], 3O4M (Crystal structure of porcine pancreatic phospholipase A2 in complex with 1,2-dihydroxybenzene)

[19], 4YRE (Crystal structure of T. cruzi Histidyl-tRNA synthetase in complex with (2-bromophenyl)methanol) [20], 7NNY (Crystal structure of Mycobacterium tuberculosis ArgF in complex with naphthalen-1-ol) [21], and 7OFS (Structure of SARS-CoV-2 Papain-like protease PLpro in complex with 4-(2-hydroxyethyl)phenol) [22].

Table 2. Native ligands and their co-crystallized PDB ID.

S. No	Compound code	Native Ligand (Co-crystallized ligand)	PDB ID
1	NL1	1,2-dihydroxybenzene	3O4M
2	NL2	4-chlorobenzene-1,2-diol	7DQL
3	NL3	naphthalen-1-ol	7NNY
4	NL4	4-(2-hydroxyethyl)phenol	7OFS
5	NL5	(2-bromophenyl)methanol)	4YRE

Preparation of ligands: The 2D representations of the compounds under study, along with the native ligands co-crystallized on the target PDBs, were transformed into 3D structures. These 3D structures underwent energy minimization utilizing the molecular mechanics 2 (MM2) force field within ChemBio3D Ultra 12.0 software. Subsequently, the optimized 3D structures were saved in the SYBYL MOL2 file format, enabling their suitability for docking simulations.

Docking: Molegro Virtual Docker (MVD 6.0) was employed for conducting the docking study [23]. MVD utilizes an internal algorithm to identify potential binding sites within protein structures, typically generating multiple cavities based on concave regions capable of accommodating ligands. Docking parameters were set with the MolDock score [GRID] and rerank score as the scoring function and a grid resolution of 0.30 Å. Binding site coordinates for each target were specified accordingly: PDB ID: 7DQL (Chain A) with a volume of 27.136 Å^3, centre X: 25.06, Y: 20.36, Z: 19.70, within a constraint of a radius of 12 Å; PDB ID: 3O4M (Chain A) having a volume of 120.32 Å^3, centre designated as X: 36.06, Y: -17.38, Z: 18.63 within a constraint of radius 12 Å; PDB ID: 4YRE (Chain A) having a volume of 345.088 Å^3, centre designated as X: 11.29, Y: -5.91, Z: 39.34 within a constraint of radius 12 Å; PDB ID: 7NNY (Chain A) having a volume of 210.94 Å^3, centre designated as X: -0.79, Y: -16.86, Z: -56.46 within a constraint of radius 12 Å; and PDB ID: 7OFS (Chain A) having a volume of 66.56 Å^3, centre designated as X: 42.59, Y: 6.76, Z: 35.50 within a constraint of radius 12 Å. Following this, detailed analysis cantered on assessing MolDock and rerank scores and elucidating the interactions between ligands and receptors. The computational parameters were standardized across all PDB IDs, with a maximum iteration limit of 1,500 and a population size capped at 50. To refine the accuracy of the docking process, each ligand underwent 30 individual

runs. Subsequent scrutiny focused on evaluating docking scores and elucidating ligand-receptor interactions [**24-28**].

Density functional theory (DFT): The top hit compounds generated from the docking study, along with the native ligands, were further investigated using density functional theory (DFT) to compute the HOMO and LUMO energy values in order to understand their reactivity and stability. The Gaussian16 [**29**] suite of programs was employed to optimize the structures, and vibrational frequency analysis was performed to ensure that the structures were at their ground state and free from any imaginary frequency. LANL2DZ basis sets were utilized to optimize the structures. The CubeGen extension within GaussView6 [**30**] was employed to generate the HOMO and LUMO orbital's and other descriptors for all structures.

Drug likeness and ADME/T screening: Underwent drug likeness screening via Swiss ADME [**31**], ensuring adherence to Lipinski, Veber, and Egan filters, and absence of PAINS alerts. Canonical SMILES representations of the compounds were used to generate the results and screened for Lipinski's Rule of 5, Veber, and Egan filters [**32**]. The ADME process involves absorption, distribution, metabolism, and excretion. In this phase, screening was conducted for skin permeation (log Kp), P-glycoprotein (P-gp) substrate, blood-brain barrier (BBB) permeability, and gastrointestinal (GI) absorption. SwissADME software was utilized for these screenings, employing standard values derived from validated experimental studies. Employing StopTox, which focuses on identifying hazard potentials from short exposure durations, compounds underwent toxicity screening. Compound SMILES were generated using specialized software and uploaded to StopTox [**32**] for screening.

<div align="center">

RESULTS AND DISCUSSION

</div>

Molecular docking: The docking results provided critical insights into the interaction between halogen-substituted compounds and their target proteins. Docking is a computational technique used to predict the binding mode and affinity of ligands (compounds) to their respective protein targets. MolDock score is a scoring function used in docking studies to assess the binding affinity of ligands to proteins, and rerank score enhances the precision of docking. A higher negative MolDock score, in compliance with rerank score, indicates stronger binding between the ligand and the protein target. Results revealed that among all the derivatives, compounds 7F, 4F, 7Br, 1F, and 7I exhibited the highest MolDock and rerank scores relative to their protein targets PDB ID 7DQL, 3O4M, 4YRE, 7NNY, and 7OFS as shown in tables 3, 4, 5, 6, and 7, respectively. Furthermore, upon comparative analysis with the parent compound gentisyl alcohol and the native ligand, these five derivatives demonstrated notably enhanced MolDock rerank scores. This highlights the importance of halogen substitutions in modulating the pharmacological properties of the compounds, potentially enhancing their therapeutic efficacy, suggesting that the halogenated derivatives of gentisyl alcohol, especially those bearing halogen substitutions, possess significant potential as antibacterial, anti-inflammatory, anti-parasitic, anti-tubercular, and antiviral agents, showcasing a broad spectrum of bioactivity.

Interaction study of the docked compounds: The study of interactions between docked ligands and their target proteins provides invaluable insights into molecular-level interactions. Such investigations are essential for comprehending how ligands engage with the active pocket of the target protein. The present interaction analysis aimed to assess whether the studied ligands exhibit similar interactions and share common residues with the native ligand at the target site. For PDB IDs 7DQL, 3O4M, 4YRE, 7NNY, and 7OFS, compounds 7F, 4F, 1F, 7Br, and 7I displayed the highest MolDock on par with rerank scores compared to the native ligands and gentisyl alcohol. Consequently, interaction studies were conducted for these ligands and their respective target proteins, alongside the native ligands. Table 8 illustrates the interacting residues for PDB ID 7DQL, revealing that 7F share Thr165 and Val71 with the native ligand (NL2), also illustrated in figure 1A and 1B. In table 9, examining PDB 3O4M, it's noted that 4F does not share similar residues with the native ligand

Table 3. Docking score of the compounds understudy along with the native ligand with PDB ID 7DQL.

Ligand	MolDock Score	[a]Rerank Score	[b]Interaction	[c]Internal	[d]HBond	[e]LE1	[f]LE3
7.F	-70.4628	-65.6483	-93.4103	22.9476	-5.82177	-5.42021	-5.04987
5.F	-72.5714	-65.6069	-90.3917	17.8203	-5.79773	-6.04762	-5.46724
5Cl	-74.6447	-63.7137	-86.9625	12.3178	-5.8212	-6.22039	-5.30947
6.F	-70.519	-63.2919	-87.6199	17.1009	-1.28428	-5.87659	-5.27433
7Cl	-73.2493	-63.2623	-87.436	14.1867	-5.62176	-5.63456	-4.86633
3.F	-72.7512	-62.9849	-84.0496	11.2984	-2.22558	-6.61375	-5.7259
1.F	-73.0575	-62.7751	-84.7883	11.7309	-5.7945	-6.64159	-5.70683
4.F	-70.4898	-62.7033	-87.7335	17.2437	-5.82175	-5.87415	-5.22527
6Cl	-70.9534	-62.5584	-84.3457	13.3923	-3.75978	-5.91279	-5.2132
6.Br	-71.8858	-62.2944	-83.5337	11.6479	-3.77016	-5.99048	-5.1912
5.Br	-74.4058	-62.1774	-84.8352	10.4294	-5.82015	-6.20049	-5.18145
6 I	-73.8062	-62.1499	-82.6073	8.80105	-3.74881	-6.15052	-5.17916
3Cl	-71.9115	-61.7287	-81.9208	10.0093	-5.23017	-6.53741	-5.6117
2 I	-71.0765	-60.8434	-81.2415	10.165	-3.96401	-6.4615	-5.53122
3.Br	-71.6115	-60.6086	-81.1864	9.57486	-5.67337	-6.51014	-5.50988
3 I	-71.1294	-59.9436	-79.8594	8.72994	-5.54653	-6.46631	-5.44942
7.Br	-72.212	-59.9328	-85.4527	13.2406	-5.82151	-5.55477	-4.61022
1Cl	-68.4207	-59.6828	-79.8163	11.3955	-5.00679	-6.22007	-5.42571
1.Br	-71.6571	-59.4586	-81.2776	9.62049	-5.82077	-6.51428	-5.40533
NL2	-67.3256	-59.2371	-76.4208	9.09519	-5.88406	-7.48063	-6.5819
Gentisyl alcohol	-66.8757	-59.1602	-74.1881	7.31239	-5.54791	-6.68757	-5.91602
2.F	-66.0272	-58.6322	-81.2373	15.2102	-5.82168	-6.00247	-5.3302
7 I	-72.0759	-58.5214	-81.5107	9.43479	-5.82197	-5.5443	-4.50164
4Br	-69.782	-58.2967	-81.3774	11.5953	-5.82134	-5.81517	-4.85806
1 I	-70.0378	-57.8883	-79.6168	9.57899	-5.18438	-6.36707	-5.26257
2Cl	-66.7151	-57.5678	-79.1778	12.4627	-5.50462	-6.06501	-5.23344
4Cl	-68.8166	-57.3128	-82.8852	14.0685	-5.82159	-5.73472	-4.77607
4 I	-69.0603	-57.1619	-77.968	8.90763	-5.74322	-5.75503	-4.76349
5 I	-70.7795	-56.1653	-80.5975	9.81798	-5.61982	-5.89829	-4.68044
2.Br	-65.59	-54.7224	-77.3757	11.7857	-5.8218	-5.96273	-4.97476

[a]Rerank score, [b]Total interaction energy (kJ mol^{-1}), [c] Internal energy, [d]Hydrogen bond (kJ mol^{-1}), [e]Ligand efficiency1, [f]Ligand efficiency3

Table 4. Docking score of the compounds understudy along with the native ligand with **PDB ID 3O4M**

Ligand	MolDock Score	[a]Rerank Score	[b]Interaction	[c]Internal	[d]HBond	[e]LE1	[f]LE3
4.F	-71.4785	-64.1709	-88.7104	17.2319	-8.83335	-5.95654	-5.34758
1F	-74.3025	-63.5966	-85.9808	11.6783	-9.37795	-6.75477	-5.78151
4Cl	-73.1747	-62.5083	-86.5354	13.3606	-9.15153	-6.09789	-5.20902
6 I	-74.6296	-62.2742	-83.65	9.02039	-9.80542	-6.21913	-5.18952
1Cl	-73.6334	-62.12	-83.8841	10.2507	-9.13806	-6.69395	-5.64728
6Br	-71.8577	-61.8909	-83.7726	11.915	-10.3074	-5.98814	-5.15758
1Br	-73.5002	-61.7015	-83.1511	9.65095	-8.98585	-6.68184	-5.60923
1 I	-73.042	-61.1701	-82.1135	9.07146	-10.5154	-6.64018	-5.56092
6Cl	-69.8085	-61.159	-83.3911	13.5827	-10.3157	-5.81737	-5.09659
4Br	-74.6667	-61.1359	-86.2614	11.5947	-10.2168	-6.22223	-5.09466
5 I	-72.3453	-60.9883	-81.1236	8.77832	-9.04221	-6.02877	-5.08236
5Br	-70.9759	-60.9084	-80.9286	9.95271	-8.83748	-5.91466	-5.0757
5F	-69.2788	-60.8901	-86.7299	17.451	-9.65363	-5.77324	-5.07418
4 I	-75.1495	-60.5237	-84.1262	8.97673	-10.1132	-6.26246	-5.04364
Gentisyl alcohol	-69.3514	-60.3189	-76.6234	7.27199	-9.80373	-6.93514	-6.03189
7F	-60.8021	-60.1955	-83.7583	22.9562	-10	-4.67709	-4.63042
7 I	-71.4452	-59.2918	-79.8452	8.39995	-6.55376	-5.49579	-4.5609
7Br	-67.1677	-59.1331	-79.8604	12.6927	-7.33557	-5.16675	-4.5487
6F	-64.7639	-59.094	-82.0247	17.2609	-8.87449	-5.39699	-4.9245
3 I	-69.1523	-58.7262	-77.9045	8.75227	-9.10798	-6.28657	-5.33875
5Cl	-72.1902	-58.5299	-84.1317	11.9415	-9.43259	-6.01585	-4.87749
3Br	-68.756	-58.3809	-77.876	9.11998	-6.06484	-6.25055	-5.30736
3Cl	-68.2285	-58.173	-77.6926	9.46415	-6.0461	-6.20259	-5.28846
7Cl	-65.391	-58.1658	-79.57	14.179	-10	-5.03008	-4.47429
3F	-66.0586	-57.7016	-77.4571	11.3984	-6.13598	-6.00533	-5.2456
2Cl	-65.2571	-57.4611	-77.6982	12.441	-7.38549	-5.93247	-5.22374
2Br	-67.0841	-57.3168	-78.3205	11.2364	-6.94903	-6.09856	-5.21062
2 I	-66.792	-56.8794	-76.2332	9.44122	-7.67612	-6.072	-5.17086
2F	-64.6764	-55.3344	-80.5942	15.9178	-8.63567	-5.87968	-5.0304
NL1	-54.6871	-49.9012	-66.1336	11.4465	-6.57237	-6.83589	-6.23765

[a]Rerank score, [b]Total interaction energy (kJ mol^{-1}), [c] Internal energy, [d]Hydrogen bond (kJ mol^{-1}), [e]Ligand efficiency1, [f]Ligand efficiency3

Table 5. Docking score of the compounds understudy along with the co-crystallized ligand with **PDB ID 4YRE**

Ligand	MolDock Score	[a]Rerank Score	[b]Interaction	[c]Internal	[d]HBond	[e]LE1	[f]LE3
1F	-77.6122	-66.2661	-89.0099	11.3978	-5.03434	-7.05565	-6.02419
2Cl	-78.2777	-66.1686	-90.8406	12.5629	-5.37026	-7.11616	-6.01533
7F	-71.7519	-65.7285	-94.6684	22.9165	-4.33829	-5.51938	-5.05604
2 I	-77.6853	-65.3122	-87.3005	9.61515	-4.55721	-7.0623	-5.93747
6F	-72.4403	-65.2636	-91.695	19.2547	-5.13668	-6.03669	-5.43863
2Br	-75.8134	-64.9217	-87.215	11.4016	-4.54579	-6.89213	-5.90197
2F	-72.6898	-64.8635	-88.0412	15.3514	-4.48116	-6.60817	-5.89669
5F	-73.7169	-64.6726	-91.3466	17.6297	-4.44498	-6.14307	-5.38939
4Cl	-73.4337	-64.5737	-87.4786	14.0449	-5.07313	-6.11948	-5.38114
4F	-72.2288	-64.2278	-89.4661	17.2373	-4.94979	-6.01907	-5.35231
Gentisyl alcohol	-72.8163	-63.3134	-82.2533	9.43707	-3.92414	-7.28163	-6.33134
4Br	-73.1637	-63.1493	-84.6806	11.5169	-5.04334	-6.09698	-5.26244
5Cl	-75.9018	-62.8429	-87.8108	11.909	-5.24905	-6.32515	-5.23691
3F	-75.4836	-62.3833	-86.8031	11.3195	-5.2614	-6.86215	-5.67121
NL5	-72.8867	-61.6306	-80.7632	7.87651	-2.5	-8.09852	-6.84784
Cl1	-71.6956	-61.0823	-81.9332	10.2376	-4.46491	-6.51778	-5.55294
Cl6	-70.2211	-60.9664	-84.2217	14.0006	-5.07568	-5.85176	-5.08054
1 I	-71.8691	-60.8673	-82.2845	10.4154	-7.4398	-6.53355	-5.53339
Cl3	-74.7331	-60.7047	-84.1731	9.44001	-5.35559	-6.79392	-5.51861
4 I	-71.9176	-59.7697	-80.9195	9.00193	-6.96512	-5.99313	-4.98081
1Br	-70.4729	-59.6567	-80.0949	9.62201	-4.34495	-6.40663	-5.42334
5Br	-71.8011	-59.3654	-83.3061	11.505	-7.11429	-5.98342	-4.94712
6.Br	-71.6027	-59.051	-83.0581	11.4554	-3.40566	-5.96689	-4.92091
7 I	-69.8574	-58.3767	-78.2599	8.40244	-9.65896	-5.37365	-4.49051
5 I	-73.9179	-58.1599	-82.6868	8.76887	-5.12291	-6.15983	-4.84665
Cl7	-66.8602	-58.0553	-84.3215	17.4614	-4.78077	-5.14309	-4.46579
7Br	-68.6993	-58.0458	-81.4227	12.7234	-11.188	-5.28456	-4.46506
3Br	-70.9891	-58.0013	-81.6089	10.6198	-6.9452	-6.45355	-5.27285
3 I	-70.7326	-57.7763	-79.4703	8.73773	-3.74692	-6.43024	-5.25239
6 I	-72.9806	-57.7031	-81.5924	8.61182	-3.4	-6.08172	-4.80859

[a]Rerank score, [b]Total interaction energy (kJ mol^{-1}), [c] Internal energy, [d]Hydrogen bond (kJ mol^{-1}), [e]Ligand efficiency1, [f]Ligand efficiency3

Table 6. Docking score of the compounds understudy along with the co-crystallized ligand with **PDB ID 7NNY**

Ligand	MolDock Score	[a]Rerank Score	[b]Interaction	[c]Internal	[d]HBond	[e]LE1	[f]LE3
7Br	-73.4757	-61.6228	-86.9809	13.5052	-9.41049	-5.65198	-4.74021
NL3	-69.036	-61.5524	-82.3051	13.2691	-2.5	-6.276	-5.59567
7Cl	-72.2875	-60.5637	-86.6541	14.3666	-9.305	-5.56058	-4.65875
4F	-68.7423	-60.5387	-85.9525	17.2102	-9.17913	-5.72852	-5.04489
7F	-64.6036	-60.3864	-90.0297	25.4261	-8.65865	-4.96951	-4.6451
7 I	-74.2003	-59.7522	-83.2668	9.0665	-8.98444	-5.70771	-4.59632
6F	-68.7985	-59.7145	-85.926	17.1275	-9.30967	-5.73321	-4.97621
Gentisyl alcohol	-67.5666	-59.2873	-74.8421	7.2755	-8.24933	-6.75666	-5.92873
4Cl	-70.1272	-59.2126	-83.4985	13.3713	-9.02367	-5.84393	-4.93438
5F	-65.4319	-58.9731	-82.9228	17.4909	-6.9353	-5.45266	-4.91443
1F	-67.8203	-58.4701	-79.4955	11.6753	-7.3217	-6.16548	-5.31546
2Br	-66.6925	-58.0626	-77.8897	11.1972	-9.09996	-6.06295	-5.27842
1Cl	-68.2937	-58.0237	-78.5227	10.229	-7.03368	-6.20852	-5.27488
Cl6	-69.05	-58.0089	-83.1496	14.0996	-9.29885	-5.75416	-4.83408
4 I	-71.3	-57.9545	-79.7675	8.46751	-8.88519	-5.94167	-4.82954
6Br	-69.8278	-57.9283	-81.563	11.7352	-9.37385	-5.81898	-4.82736
1Br	-68.5094	-57.9051	-78.1439	9.63444	-6.96236	-6.22813	-5.2641
2 I	-68.2615	-57.8421	-77.0867	8.82522	-8.83096	-6.20559	-5.25837
3F	-69.5895	-57.4601	-81.3371	11.7477	-9.28316	-6.32631	-5.22364
4Br	-68.5305	-57.3763	-80.4653	11.9348	-9.31339	-5.71087	-4.78136
5Br	-67.2605	-56.9265	-77.5072	10.2467	-7.71109	-5.60504	-4.74388
1 I	-67.6619	-56.8633	-76.749	9.08711	-6.8827	-6.15108	-5.16939
2Cl	-64.8843	-56.6145	-77.8605	12.9762	-10.5972	-5.89858	-5.14677
3Cl	-70.244	-56.4473	-80.1207	9.87673	-9.28169	-6.38582	-5.13157
3Br	-69.5534	-55.9859	-79.0206	9.46721	-9.17558	-6.32303	-5.08963
2F	-63.7513	-55.6793	-78.9572	15.2059	-9.77021	-5.79557	-5.06175
5Cl	-65.4088	-55.0807	-77.6217	12.2128	-8.94345	-5.45074	-4.59006
6 I	-67.9268	-54.6134	-75.9178	7.99101	-5.08904	-5.66057	-4.55112
5 I	-66.0541	-53.8953	-75.1481	9.09401	-7.61317	-5.50451	-4.49127
3 I	-63.4395	-52.4566	-74.7244	11.2849	-7.71831	-5.76723	-4.76878

[a]Rerank score, [b]Total interaction energy (kJ mol^{-1}), [c] Internal energy, [d]Hydrogen bond (kJ mol^{-1}), [e]Ligand efficiency1, [f]Ligand efficiency3
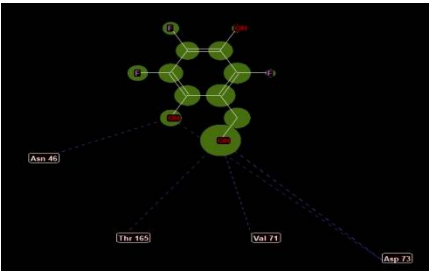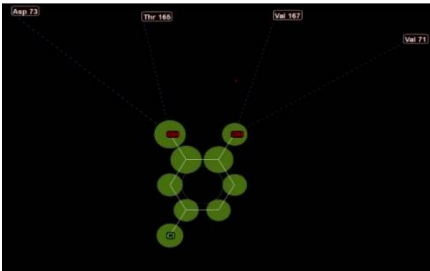
Table 7. Docking score of the compounds understudy along with the co-crystallized ligand with **PDB ID 7OFS.**

Ligand	MolDock Score	[a]Rerank Score	[b]Interaction	[c]Internal	[d]HBond	[e]LE1	[f]LE3
7 I	-82.2235	-68.1329	-91.7848	9.56132	-9.29862	-6.32489	-5.24099
NL4	-78.9391	-67.9609	-85.1029	6.16384	-4.85818	-7.89391	-6.79609
5Cl	-74.4179	-67.8277	-91.9548	17.5368	-10.0593	-6.20149	-5.6523
4F	-75.564	-67.7576	-92.7712	17.2071	-8.21206	-6.297	-5.64647
7Br	-78.6958	-67.4568	-91.6596	12.9639	-8.58233	-6.05352	-5.18898
7Cl	-77.4249	-66.8503	-91.579	14.154	-8.1243	-5.95576	-5.14233
5F	-72.7737	-66.8458	-90.4026	17.6289	-4.04249	-6.06448	-5.57049
4Br	-77.1484	-66.5823	-88.8715	11.7231	-10.2082	-6.42903	-5.54853
5Br	-78.2318	-66.3815	-88.2782	10.0464	-4.27472	-6.51932	-5.5318
6 I	-80.4923	-66.1831	-88.4531	7.96071	-7.60343	-6.7077	-5.51526
4 I	-80.0177	-66.1625	-88.2878	8.27009	-7.98051	-6.66815	-5.51354
7F	-68.5016	-65.7634	-91.8764	23.3748	-7.39549	-5.26935	-5.05872
6Br	-78.2992	-65.5591	-89.6193	11.32	-7.65224	-6.52494	-5.46326
1F	-76.5402	-65.2239	-88.2081	11.668	-8.47902	-6.9582	-5.92945
5 I	-76.3179	-65.1968	-88.2919	11.974	-8.93125	-6.35982	-5.43306
1Cl	-76.5867	-64.4931	-86.8185	10.2318	-8.6776	-6.96243	-5.86301
4Cl	-73.3926	-64.0162	-86.6971	13.3046	-8.12743	-6.11605	-5.33469
2F	-70.5651	-63.7715	-85.8142	15.249	-4.91977	-6.41501	-5.79741
1Br	-76.0694	-63.7132	-85.6891	9.61969	-8.74588	-6.9154	-5.79211
6F	-73.4738	-63.5666	-90.5982	17.1244	-4.95443	-6.12282	-5.29721
3F	-73.5263	-63.3952	-85.2737	11.7474	-4.4313	-6.68421	-5.7632
6Cl	-72.3967	-63.2652	-85.7224	13.3257	-9.39264	-6.03306	-5.2721
Gentisyl alcohol	-72.0798	-63.2432	-79.3546	7.27477	-5.48439	-7.20798	-6.32432
3Cl	-73.9985	-62.8006	-83.9689	9.97043	-2.8086	-6.72713	-5.70915
3 I	-73.6983	-62.7672	-83.7807	10.0823	-3.85488	-6.69985	-5.70611
3Br	-74.1524	-62.6513	-83.6095	9.45709	-3.97088	-6.74113	-5.69557
1 I	-74.3596	-62.4431	-83.3816	9.022	-10.1454	-6.75996	-5.67664
2 I	-74.7751	-62.2444	-83.5592	8.78404	-8.94574	-6.79774	-5.65858
2Br	-72.0048	-62.0882	-83.2212	11.2165	-5.16072	-6.54589	-5.64438
2Cl	-71.1398	-62.0512	-83.5597	12.4198	-5.15843	-6.46726	-5.64102

[a]Rerank score, [b]Total interaction energy (kJ mol^{-1}), [c] Internal energy, [d]Hydrogen bond (kJ mol^{-1}), [e]Ligand efficiency1, [f]Ligand efficiency3
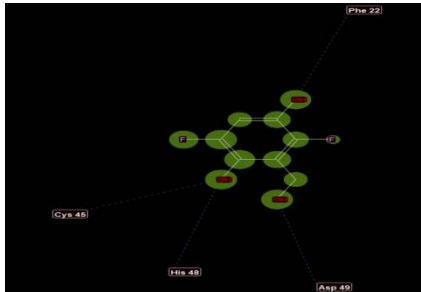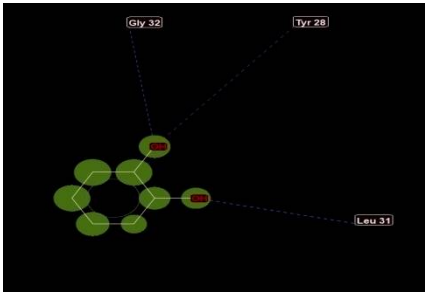
depicted in figure 2A and 2B. Moving to table 10 for PDB ID 4YRE, it is observed that 1F and NL5 both interact with Trp155, as shown in figure 3A and 3B. Similarly, table 11 presents the interactingresidues for PDB ID 7NNY, where 7Br and NL3 share Gln231, shown in figure 4A and 4B. Lastly, in table 12 for PDB ID 7OFS, it is evident that 7I and NL4 both interact with Asp76, shown in figure 5A and 5B. These findings shed light on the specific residues involved in ligand-

Table 8. Molecular Interaction Between the ligand inhibitor and target PDB 7DQL.
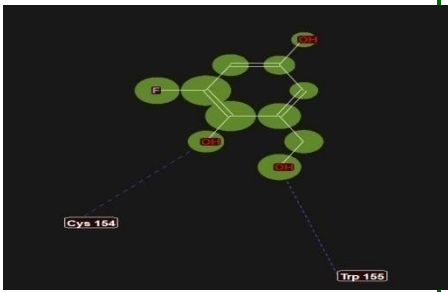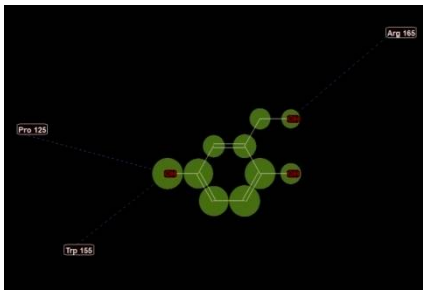
Ligand inhibitor	Interacting residue	Ligand inhibitor	Interacting residue
	Asn46, Thr165, Val71, Asp73		Asp73, Thr165, Val167, Val71
7F	Figure 1A. 7F.	NL2	Figure 2A. NL2.

protein interactions, aiding in understanding the binding mechanisms and potential modes of action of the studied compounds. Moreover, identifying common residues between the ligands and native ligands provides insights into the structural features contributing to their binding affinity and biological activity, which are crucial for rational drug design and optimization [34].
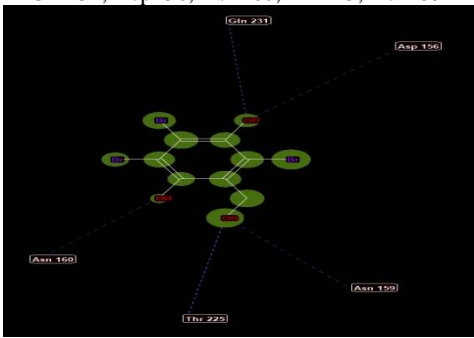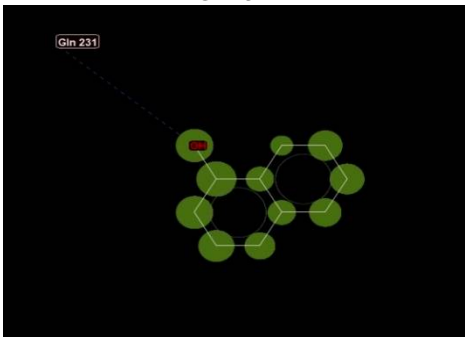
Table 9. Molecular Interaction Between the ligand inhibitor and target PDB **3O4M**

Ligand inhibitor	Interacting residue	Ligand inhibitor	Interacting residue
4F	Phe22, Cys45, His48, Asp49 **Figure 2A. 1F.**	NL1	Gly32, Tyr28, Leu31 **Figure 2B. NL1.**

Table 10. Molecular Interaction Between the ligand inhibitor and target PDB **4YRE.**

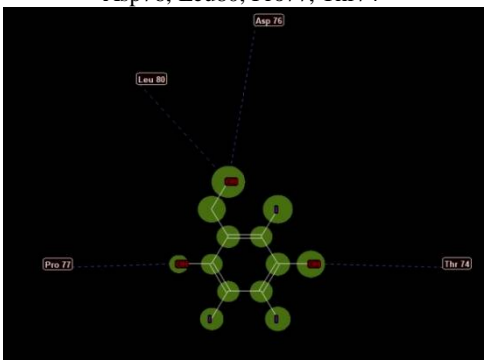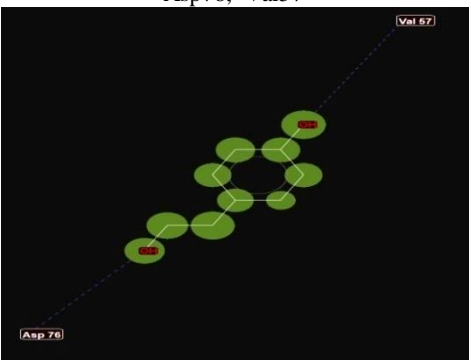| Ligand inhibitor	Interacting residue	Ligand inhibitor	Interacting residue
`1F	Cys154, Trp155 **Figure 3A**. 1F	NL5	Pro125, Trp155, Arg165 **Figure.** 3B:NL5.

Table 11. Molecular Interaction Between the ligand inhibitor and target PDB **7NNY.**

Ligand inhibitor	Interacting residue	Ligand inhibitor	Interacting residue
7Br	Gln231, Asp156, Asn160, Thr225, Asn159 **Figure 4A.** 7Br	NL3	Gln231 **Figure 4B.** NL3

Table 12. Molecular Interaction Between the ligand inhibitor and target PDB **7OFS.**

Ligand inhibitor	Interacting residue	Ligand inhibitor	Interacting residue
7I	Asp76, Leu80, Pro77, Thr74 **Figure 5A.** 7I	NL4	Asp76, Val57 **Figure 5B.** NL4

Density functional theory (DFT): Understanding the HOMO-LUMO energy gap is crucial in drug design and optimization. A smaller gap indicates a more reactive molecule, which may be advantageous in certain therapeutic applications such as drug delivery or catalysis. Conversely, a larger gap suggests a more stable molecule, which may be desirable for maintaining drug efficacy or minimizing side effects. Specifically, as shown in table 13 and illustrated in figure 6, the order of the HOMO-LUMO energy gap (7I > 7Br > NL3 > 4F > 7F > 1F > NL4 > NL1 > NL2 > NL5) suggests that 7I may exhibit the highest reactivity and stability, while NL5, characterized by a larger HOMO-LUMO gap, could possess lower reactivity and stability compared to the other compounds. This finding is significant as it provides insights into the potential chemical reactivity and stability of the compounds. These findings offer valuable guidance for further exploration and optimization of the compounds for therapeutic use.

Druglikeness and ADME/T screening: According to the druglikeness rule of five, an orally active drug should not violate more than one of the implemented criteria. Upon druglikeness screening, it is evident that, except for the native ligand 7I, which exhibits one violation for the Lipinski rule, all other compounds under study demonstrate zero violations, indicating their druglike characteristics. In ADME screening, all compounds exhibit high gastrointestinal absorption, a favourable trait. None of the compounds are found to be blood-brain barrier permeable, implying limited access to the central nervous system. Additionally, none of the compounds show substrate activity to P-glycoprotein, a protein associated with drug resistance. Skin permeability, measured by

Table 13. Calculated HOMO-LUMO energy gap via DFT

Compound	Homo	Lumo	Homo-Lumo (in H)	Homo-Lumo (in eV)
NL 1	-0.22123	-0.01054	0.21069	5.733169866
NL 2	-0.23289	-0.02661	0.20628	5.613167592
NL 3	-0.20976	-0.04053	0.16923	4.604985222
NL 4	-0.22577	-0.01512	0.21065	5.73208141
NL 5	-0.25902	-0.03428	0.22474	6.115490036
1F	-0.22171	-0.01917	0.20254	5.511396956
4F	-0.23665	-0.04193	0.19472	5.298603808
7F	-0.24834	-0.04778	0.20056	5.457518384
7Br	-0.23711	-0.07139	0.16572	4.509473208
7I	-0.23048	-0.08919	0.14129	3.844698706
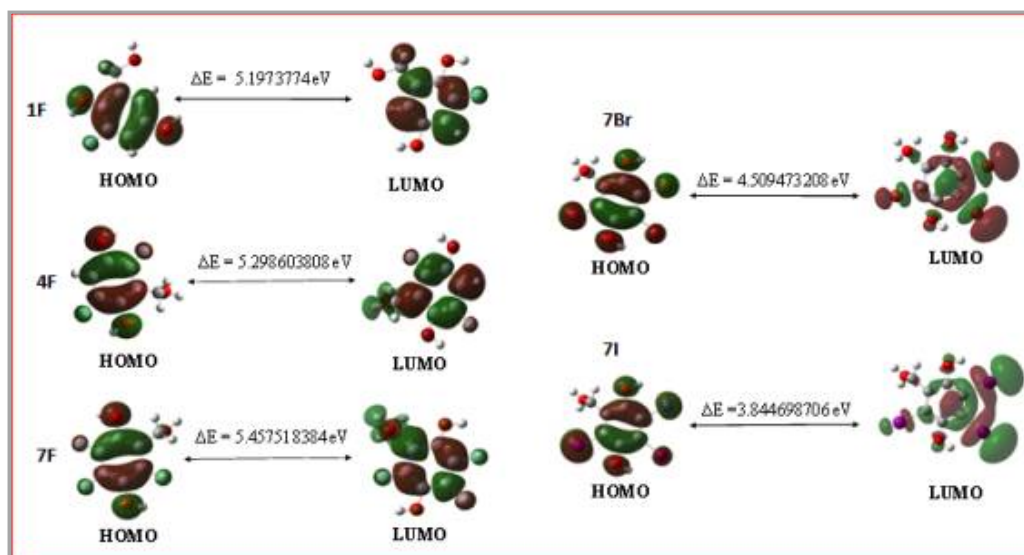
Figure 6. Cartoon illustration of the HOMO-LUMO gap of 7F, 4F, 7Br, 1F, and 7I .

log KP values ranging from -5.51 to -7.45, indicates moderate skin permeability for all compounds. In toxicity screening, the top hit compounds—1F, 4F, 7F, 7I, and 7Br—along with the parent compound gentisyl alcohol, display negative results for acute inhalation toxicity, eye irritation, and skin irritation. Conversely, native ligands exhibit at least one toxic variation. Overall, the top hit compounds demonstrate favorable druglike characteristics, as well as well-announced pharmacokinetics and toxicity properties, based on druglikeness and ADME/T screening results.

Table 14. Druglikness and ADME/ screening via SwissADME and StopTox.

Compound ID	Adme Screening				Druglikeness Screening				Toxicity		
	GI absorption	BBB permeant	P-gp substrate	Log K_p (skin permeation) (cm s^{-1})	Lipinski	Veber	Egan	Bioavailability Score	Acute Inhalation Toxicity	Eye Irritation and Corrosion	Skin Irritation and Corrosion
GA	High	No	No	-6.68	Yes; 0 violation	Yes	Yes	0.55	Non Toxic	Non Toxic	Negative
1F	High	Yes	No	-6.50	Yes; 0 violation	Yes	Yes	0.55	Non Toxic	Non Toxic	Negative
4F	High	Yes	No	-6.61	Yes; 0 violation	Yes	Yes	0.55	Non Toxic	Non Toxic	Negative
7F	High	Yes	No	-6.65	Yes; 0 violation	Yes	Yes	0.55	Non Toxic	Non Toxic	Negative
7I	High	Yes	No	-7.45	Yes; 1 violation: MW>500	Yes	Yes	0.55	Non Toxic	Non Toxic	Negative
7Br	High	Yes	No	-6.50	Yes; 0 violation	Yes	Yes	0.55	Non Toxic	Non Toxic	Negative
NL1	High	Yes	No	-6.35	Yes; 0 violation	Yes	Yes	0.55	Toxic	Toxic	Negative
NL2	High	Yes	No	-5.51	Yes; 0 violation	Yes	Yes	0.55	Toxic	Toxic	Negative
NL3	High	Yes	No	-5.16	Yes; 0 violation	Yes	Yes	0.55	Non Toxic	Toxic	Negative
NL4	High	Yes	No	-6.84	Yes; 0 violation	Yes	Yes	0.55	Non Toxic	Toxic	Positive
NL5	High	Yes	No	-6.57	Yes; 0 violation	Yes	Yes	0.55	Toxic	Toxic	Positive

APPLICATION

The findings of this study hold significant implications for the development of novel therapeutic agents targeting antimicrobial resistance (AMR) and inflammation-related conditions. By incorporating halogen atoms into gentisyl alcohol, the study aims to enhance the molecule's properties and assess its potential as an antibacterial, anti-tubercular, antiviral, anti-parasitic, and anti-inflammatory agent. Overall, this research offers a promising avenue for the development of broad-spectrum therapeutic agents to address the dual challenges of AMR and inflammation-related diseases.

CONCLUSION

In conclusion, addressing antimicrobial resistance (AMR) alongside inflammation highlights the urgent need for innovative therapeutic strategies. Halogenation, as a means to modify molecular properties, shows significant potential in drug development by impacting bioactivity and metabolism. This study aimed to design variations of gentisyl alcohol with bromine, fluorine, chlorine, and iodine atoms, evaluating their multifaceted potential across antibacterial, anti-tubercular, antiviral, anti-parasitic, and anti-inflammatory activities. Using advanced computational techniques, including molecular docking and Density Functional Theory (DFT) studies, we assessed the binding affinity, reactivity, and stability of these compounds. Our findings revealed that compounds 7F, 4F, 7Br, 1F, and 7I exhibited exceptional docking scores, surpassing gentisyl alcohol and native ligands against specific targets. Furthermore, DFT analysis indicated their superior stability and reactivity compared to native ligands. These compounds also demonstrated favorable drug-like characteristics, including adherence to the rule of five and promising results in ADME/T screening. Additionally, they exhibited high gastrointestinal absorption, limited blood-brain barrier permeability, and minimal toxicity, highlighting their potential as lead compounds for drug development. In summary, the identified compounds show promise for further exploration and optimization in therapeutic applications, offering multifunctional benefits in combating both antimicrobial resistance and inflammation.

ACKNOWLEDGMENT

REFERENCES

[1]. Global Health Estimates. https://www.who.int/data/global-health-estimates/
[2]. A. Wilder-Smith and S. Osman, Public health emergencies of international concern: a historic overview, *Journal of Travel Medicine*, **2020**, 27(8), doi: 10.1093/jtm/taaa227.
[3]. Antimicrobial resistance, Nov. 21, 2023. https://www.who.int/news-room/fact-sheets/ detail/ antimicrobial-resistance
[4]. D. Furman, J. Chang, L. Lartigue, C. R. Bolen, F. Haddad, B. Gaudilliere, E. A. Ganio, G. K. Fragiadakis, M. H. Spitzer, I. Douchet, S. Daburon, J.-F. Moreau, G. P. Nolan, P. Blanco, J. Déchanet-Merville, C. L. Dekker, V. Jojic, C. J. Kuo, M. M. Davis, and B. Faustin, Expression of specific inflammasome gene modules stratifies older individuals into two extreme clinical and immunological states, *Nature Medicine*, **2017**, 23(2), 174–184, doi: 10.1038/nm.4267D.

[5]. D. Furman, J. Campisi, E. Verdin, P. Carrera-Bastos, S. Targ, C. Franceschi, L. Ferrucci, D. W. Gilroy, A. Fasano, G. W. Miller, A. H. Miller, A. Mantovani, C. M. Weyand, N. Barzilai, J. J. Goronzy, T. A. Rando, R. B. Effros, A. Lucia, N. Kleinstreuer, and G. M. Slavich, Chronic inflammation in the etiology of disease across the life span, *Nature Medicine*, **2019**, 25(12), 1822–1832, Dec., doi: 10.1038/s41591-019-0675-0.

[6]. R. J. Mumper, C. G. Smith, J. T. O'Donnell, The Process of New Drug Discovery and Development, 2nd Edition, *Drug Development and Industrial Pharmacy*, **2008**, 34(11), 1267–1267, doi: 10.1080/03639040802071844.

[7]. [7]. T. Usha, D. Shanmugarajan, A. K. Goyal, C. S. Kumar, and S. K. Middha, Recent Updates on Computer-aided Drug Discovery: Time for a Paradigm Shift, *Current Topics in Medicinal Chemistry*, **2018**, 17(30), 3296–3307, doi: 10.2174/1568026618666 180101163651.

[8]. N. Dhingra, Computer-Aided Drug Design and Development: An Integrated Approach, *Drug Development Life Cycle*, **2022**, doi: 10.5772/intechopen.105003

[9]. M. Hernandes, S. M. Cavalcanti, D. R. Moreira, W. de Azevedo Junior, A. C. Leite, Halogen Atoms in the Modern Medicinal Chemistry: Hints for the Drug Design, *Current Drug Targets*, **2010**, 11(3), 303–314, doi: 10.2174/138945010790711996.

[10]. Z. Xu, Z. Yang, Y. Liu, Y. Lu, K. Chen, and W. Zhu, Halogen Bond: Its Role beyond Drug–Target Binding Affinity for Drug Discovery and Development, *Journal of Chemical Information and Modeling*, **2014**, 54(1), 69–78, doi: 10.1021/ci400539q.

[11]. Y. Lu, Y. Liu, Z. Xu, H. Li, H. Liu, and W. Zhu, Halogen bonding for rational drug design and new drug discovery, *Expert Opinion on Drug Discovery*, 2012, 7(5), 375–383, 2012, doi: 10.1517/17460441.2012.678829.

[12]. S. Jiang, L. Zhang, D. Cui, Z. Yao, B. Gao, J. Lin, and D. Wei, The Important Role of Halogen Bond in Substrate Selectivity of Enzymatic Catalysis, *Scientific Reports*, **2016**, 6(1), doi: 10.1038/srep34750.

[13]. Y. Lu, Y. Liu, Z. Xu, H. Li, H. Liu, and W. Zhu, Halogen bonding for rational drug design and new drug discovery, *Expert Opinion on Drug Discovery*, **2012**, 7(5), 375–383, doi: 10.1517/17460441.2012.678829.

[14]. S. M. S. M. Y. Subhrojyoti Narayan Roy, Emergence of Drug Discovery in Machine Learning, in Technical Advancements of Machine Learning in Healthcare, Springer link, **202**1, 119-138.

[15]. H.S. Wang, H.J. Li, L.F. Wang, Z.L. Shen, Y.C. Wu, Regioselective synthesis of gentisyl alcohol-type marine natural products, *Natural Product Research*, **2019**, 33(13), 1891-1896. doi: 10.1080/14786419.2018.1478831.

[16]. R. Wilcken, M. O. Zimmermann, A. Lange, A. C. Joerger, F. M. Boeckler, Principles and Applications of Halogen Bonding in Medicinal Chemistry and Chemical Biology, *Journal of Medicinal Chemistry*, **2013**, 56(4), 1363–1388, doi: 10.1021/jm3012068.

[17]. Z. Ul Haq, R. Uddin, L. K. Wai, A. Wadood, and N. H. Lajis, Docking and 3D-QSAR modeling of cyclin-dependent kinase 5/p25 inhibitors, *Journal of Molecular Modeling*, **2010**, 17(5), 1149–1161, doi: 10.1007/s00894-010-0817-2.

[18]. Y. Yu, J. Guo, Z. Cai, Y. Ju, J. Xu, Q. Gu, and H. Zhou, Identification of new building blocks by fragment screening for discovering GyrB inhibitors, *Bioorganic Chemistry*, **202**1, 114, 105040, doi: 10.1016/j.bioorg.2021. 105040.

[19]. K. V. Dileep, I. Tintu, P. K. Mandal, P. Karthe, M. Haridas, C. Sadasivan, Binding to PLA2 May Contribute to the Anti-Inflammatory Activity of Catechol, *Chemical Biology and Drug Design*, **2011**, 79(1), 143–147, doi: 10.1111/j.1747-0285.2011.01258.x.

[20]. C. Y. Koh, L. Kallur Siddaramaiah, R. M. Ranade, J. Nguyen, T. Jian, Z. Zhang, J. R. Gillespie, F. S. Buckner, C. L. M. J. Verlinde, E. Fan, and W. G. J. Hol, A binding hotspot inTrypanosomacruzihistidyl-tRNA synthetase revealed by fragment-based crystallographic cocktail screens, *Acta Crystallographica Section D Biological Crystallography*, 2015, 71(8), 1684–1698, doi: 10.1107/s1399004715007683.

[21]. P. Gupta, S. E. Thomas, S. A. Zaidan, M. A. Pasillas, J. Cory-Wright, V. Sebastián-Pérez, A. Burgess, E. Cattermole, C. Meghir, C. Abell, A. G. Coyne, W. R. Jacobs, T. L. Blundell, S. Tiwari, and V. Mendes, A fragment-based approach to assess the ligandability of ArgB, ArgC,

ArgD and ArgF in the L-arginine biosynthetic pathway of Mycobacterium tuberculosis," *Computational and Structural Biotechnology Journal*, **2021**, 19, 3491–3506, doi:10.1016/j.csbj.2021.06.006.

[22]. V. Srinivasan, H. Brognaro, P. R. Prabhu, E. E. de Souza, S. Günther, P. Y. A. Reinke, T. J. Lane, H. Ginn, H. Han, W. Ewert, J. Sprenger, F. H. M. Koua, S. Falke, N. Werner, H. Andaleeb, N. Ullah, B. A. Franca, M. Wang, A. L. C. Barra, M. Perbandt, M. Schwinzer, C. Schmidt, L. Brings, K. Lorenzen, R. Schubert, R. R. G. Machado, E. D. Candido, D. B. L. Oliveira, E. L. Durigon, S. Niebling, A. S. Garcia, O. Yefanov, J. Lieske, L. Gelisio, M. Domaracky, P. Middendorf, M. Groessler, F. Trost, M. Galchenkova, A. R. Mashhour, S. Saouane, J. Hakanpää, M. Wolf, M. G. Alai, D. Turk, A. R. Pearson, H. N. Chapman, W. Hinrichs, C. Wrenger, A. Meents, and C. Betzel, Antiviral activity of natural phenolic compounds in complex at an allosteric site of SARS-CoV-2 papain-like protease, *Communications Biology*, 2022, 5(1), doi: 10.1038/s42003-022-03737-7.

[23]. W. F. de Azevedo, in *Docking screens for drug discovery*, Springer, **2019**.

[24]. W. L. M. Alencar, T. da Silva Arouche, A. F. G. Neto, T. de Castro Ramalho, R. N. de Carvalho Júnior, and A. M. de Jesus Chaves Neto, Publisher Correction: Interactions of Co, Cu, and non-metal phthalocyanines with external structures of SARS-CoV-2 using docking and molecular dynamics, *Scientific Reports*, **2022**, 12(1), doi: 10.1038/s41598-022-08312-y.

[25]. V. R. Shah, J. D. Bhaliya, and G. M. Patel, In silico approach: docking study of oxindole derivatives against the main protease of COVID-19 and its comparison with existing therapeutic agents, *Journal of Basic and Clinical Physiology and Pharmacology*, **2021**, 32(3), 197–214, doi: 10.1515/jbcpp-2020-0262.

[26]. Z. Ya'u Ibrahim, A. Uzairu, G. Shallangwa, and S. Abechi, Molecular docking studies, drug-likeness and in-silico ADMET prediction of some novel β-Amino alcohol grafted 1,4,5-trisubstituted 1,2,3-triazoles derivatives as elevators of p53 protein levels, *Scientific African*, **2020**, 10. e00570, doi: 10.1016/j.sciaf.2020.e00570.

[27]. R. Thomsen and M. H. Christensen, "MolDock: A New Technique for High-Accuracy Molecular Docking," *Journal of Medicinal Chemistry*, **2006**, 49(11), 3315–3321, doi: 10.1021/jm051197e.

[28]. A. Ranjbar, M. Jamshidi and S. Torabi, Molecular modelling of the antiviral action of Resveratrol derivatives against the activity of two novel SARS CoV-2 and 2019-nCoV receptors, *Eur. Rev. Med. Pharmacol. Sci,* **2020**, 24(14),. 7834--7844.

[29]. M. J. Frisch, G. W. Trucks, H. B. Schlegel, G. E. Scuseria, M. A. Robb, J. R. Cheeseman, G. Scalmani, V. Barone, G. A. Petersson, H. Nakatsuji, X. Li, M. Caricato, A. V. Marenich, J. Bloino, B. G. Janesko, R. Gomperts, B. Mennucci, H. P. Hratchian, J. V. Ortiz, A. F. Izmaylov, J. L. Sonnenberg, D. Williams-Young, F. Ding, F. Lipparini, F. Egidi, J. Goings, B. Peng, A. Petrone, T. Henderson, D. Ranasinghe, V. G. Zakrzewski, J. Gao, N. Rega, G. Zheng, W. Liang, M. Hada, M. Ehara, K. Toyota, R. Fukuda, J. Hasegawa, M. Ishida,T. Nakajima, Y. Honda, O. Kitao, H. Nakai, T. Vreven, K. Throssell, J. A. Montgomery, Jr., J. E. Peralta, F. Ogliaro, M. J. Bearpark, J. J. Heyd, E. N. Brothers, K. N. Kudin, V. N. Staroverov, T. A. Keith, R. Kobayashi, J. Normand, K. Raghavachari, A. P. Rendell, J. C. Burant, S. S. Iyengar, J. Tomasi, M. Cossi, J. M. Millam, M. Klene, C. Adamo, R. Cammi, J. W. Ochterski, R. L. Martin, K. Morokuma, O. Farkas, J. B. Foresman, and D. J. Fox, Gaussian, Inc., Wallingford CT, 2016, Gaussian 16, Revision C.01, https://gaussian.com/gaussian16/

[30]. R.Dennington, T. Keith, and J.Millam, Semichem Inc, *Shawnee Mission KS, GaussView, Version,* 2009, 5, https://gaussian.com/gaussview6/

[31]. A. Daina, O. Michielin, and V. Zoete, SwissADME: a free web tool to evaluate pharmacokinetics, drug-likeness and medicinal chemistry friendliness of small molecules, *Scientific Reports*, 2017, 7(1), doi: 10.1038/srep42717, http://www.swissadme.ch/

[32]. C. A. Lipinski, F. Lombardo, B. W. Dominy, P. J. Feeney, Experimental and computational approaches to estimate solubility and permeability in drug discovery and development settings, *Advanced Drug Delivery Reviews*, **1997**, 23(1–3), 3-25, doi: 10.1016/s0169-409x(96)00423-1.

[33]. J. V. B. Borba, V. M. Alves, R. C. Braga, D. R. Korn, K. Overdahl, A. C. Silva, S. U. S. Hall, E. Overdahl, N. Kleinstreuer, J. Strickland, D. Allen, C. H. Andrade, E. N. Muratov, and A. Tropsha, STopTox: An in Silico Alternative to Animal Testing for Acute Systemic and Topical Toxicity, *Environmental Health Perspectives*, **2022**, 130(2), doi: 10.1289/ehp9341, https://stoptox.mml.unc.edu/

[34]. X.-Y. Meng, H.-X. Zhang, M. Mezei, and M. Cui, Molecular Docking: A Powerful Approach for Structure-Based Drug Discovery, *Current Computer Aided-Drug Design*, **2011**, 7(2), 146–157, doi: 10.2174/157340911795677602.